CHEMISTRY
A EUROPEAN JOURNAL

COMMUNICATION

DOI: 10.1002/chem.201302618

Hybrid Assemblies Based on a Gadolinium-Containing Polyoxometalate and a Cationic Polymer with Spermine Side Chains for Enhanced MRI Contrast Agents**

Wenqiang Chai,[a] Shan Wang,[b] Hang Zhao,[c] Guifeng Liu,[c] Karl Fischer,[a] Haolong Li,*[b] Lixin Wu,[b] and Manfred Schmidt*[a]

Magnetic resonance imaging (MRI) is one of the most impressive medical imaging techniques currently in use owing to its noninvasive feature and high spatial resolution.[1] Its signal is generated by the relaxation of water protons in tissues. To improve the MRI sensitivity, various magnetic materials are used as contrast agents to accelerate the relaxation of protons and enhance the MRI signals.[2] Gadolinium ions (Gd^{3+}) are generally chosen as T_1 contrast agents because of their large paramagnetic moment and long electronic relaxation time, which can effectively shorten the longitudinal relaxation time (T_1) of water protons, thus enhancing the T_1 relaxivity (r_1) and realizing a brighter contrast.[3] Currently, the most studied Gd^{3+}-based contrast agents are Gd^{3+} chelates, for example, the clinically applied gadopentetic acid. Recently, Gd^{3+} ions have also been incorporated into nanostructured assemblies and materials, such as dendrimers, liposomes, fullerenes, carbon nanotubes, nanoparticles, and metal–organic frameworks, to fabricate new Gd^{3+}-based MRI contrast agents with improved imaging performance and better biocompatibility.[4]

Polyoxometalates (POMs) comprise a large class of anionic metal–oxide clusters with well-defined structures and versatile functionalities in catalysis, electronics, and magnetics.[5] Similar to the conventional metal–organic chelates, the lacunary POMs can serve as inorganic multidentate ligands for paramagnetic metal ions like rare earth Gd^{3+}, forming a series of magnetic clusters, such as $[GdW_{10}O_{36}]^{9-}$, $[Gd(PW_{11}O_{39})_2]^{11-}$, $[Gd(BW_{11}O_{39})_2]^{15-}$, and $[Gd(CuW_{11}O_{39})_2]^{17-}$.[6] These Gd^{3+}-containing POMs (Gd-POM) have been reported to exhibit higher r_1 than the commercial contrast agent gadopentetic acid, owing to the large molecular weight and rigid framework structure of POMs that benefit the realization of a long rotational correlation time and an enhanced r_1.[6a,b] Therefore, Gd-POMs are suitable nanocarriers of Gd^{3+} for fabricating new T_1 contrast agents. However, the negatively charged surface of Gd-POMs can strongly adhere to the positively charged biological molecules, which influences the biocompatibility of Gd-POMs as contrast agents in clinical use.[7] Meanwhile, the r_1 values of Gd-POMs need to be further increased to satisfy the increasing requirement of high sensitive MRI. In this context, it is necessary to develop an efficient strategy to improve both the biocompatibility and the r_1 of Gd-POMs.

Supramolecular assembly through noncovalent interactions is a facile route to combine the building blocks with complementary properties to create synergetic functions.[8] Due to the negatively charged surfaces, POMs have been widely assembled with cationic organic molecules and polymers to construct hybrid nanostructures and materials.[9] Inspired by these works, we prepared organic–inorganic hybrid assemblies of a representative Gd-POM ($[GdW_{10}O_{36}]^{9-}$, GdW) and a cationic polymer (poly(hexylspermine)acrylamide, PHSAM) by electrostatic interaction in aqueous solution (Scheme 1) and evaluated the MRI performance of the assemblies. This design is based on the consideration that the spermine groups on the side chains of PHSAM can make the hybrid assemblies biocompatible; meanwhile, anchoring GdW clusters on the hydrophilic chains of PHASM can lead to a long rotational correlation time and does not block the exchange between bulk water and the coordinated water of GdW, thus realizing an enhanced r_1. As expected, the hybrid assemblies are well biocompatible and exhibit an enhanced MRI contrast compared with the pristine GdW.

PHSAM with a degree of polymerization of 155 and a PDI value of 1.15 was synthesized by reversible addition–fragmentation chain transfer (RAFT) polymerization. The detailed synthetic procedures and characterization results of PHSAM are shown in the Supporting Information (Figures S1–S7). Due to the hydrophilic side chains, PHSAM is well soluble in water. Dynamic light scattering (DLS) results

[a] Dr. W. Chai, Dr. K. Fischer, Prof. M. Schmidt
Institute of Physical Chemistry, University of Mainz
Jakob-Welder Weg 11, 55099 Mainz (Germany)
E-mail: mschmidt@uni-mainz.de

[b] S. Wang, Dr. H. Li, Prof. L. Wu
State Key Laboratory of Supramolecular Structure and Materials
College of Chemistry, Jilin University
Changchun 130012 (P. R. China)
E-mail: hl_li@jlu.edu.cn

[c] H. Zhao, G. Liu
China-Japan Union Hospital of Jilin University
Changchun 130012 (P. R. China)

[**] MRI = magnetic resonance imaging

Supporting information for this article is available on the WWW under http://dx.doi.org/10.1002/chem.201302618.

© 2013 Wiley-VCH Verlag GmbH & Co. KGaA, Weinheim

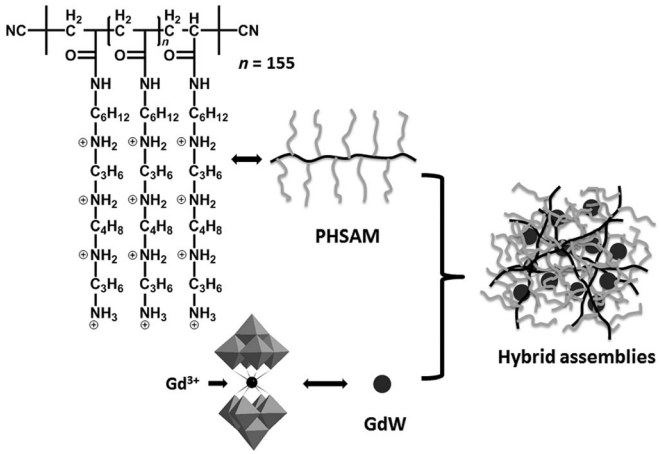

Scheme 1. Schematic illustration of the formation process of hybrid assemblies based on PHSAM and GdW.

show that either PHSAM or GdW is not able to form large assemblies in water in the investigated concentration range. The R_h value of PHSAM is around 9.8 nm (Figure S6). On the other hand, static light scattering (SLS) results show that the R_g value of PHSAM is about 17.8 nm (Figure S7). The R_g/R_h value is 1.82, which is typical for expanded coil structures in a good solvent.[10]

The PHSAM/GdW assemblies were prepared by adding the aqueous solution of GdW dropwise into the aqueous solution of PHSAM (detailed procedures are shown in the Supporting Information). After adding GdW, the solution became turbid, which indicated the formation of large assemblies. The scattering intensity gradually increased when the charge ratios of GdW to PHSAM (defined as r) were increased from 0.06, 0.08, 0.1, 0.2, and 0.3 to 0.5. However, upon further increasing r up to 1, the mixture became unstable and tended to precipitate, which may be attributed to the increasing neutralization of the positive charges of PHSAM by the anionic GdW clusters. Apparently, the residual charges on the surface of PHSAM/GdW assemblies are not sufficient to stabilize the assemblies. In situ atomic force microscopy (AFM) and cryo-TEM images both revealed that spherical PHSAM/GdW assemblies are formed in the solution (Figure 1).

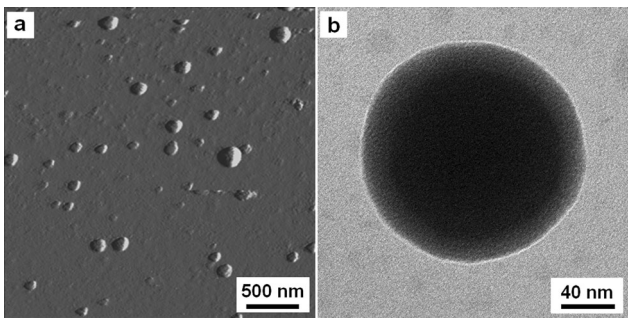

Figure 1. a) In situ AFM and b) cryo-TEM images of PHSAM/GdW assemblies with $r=0.5$ in aqueous solution.

DLS results revealed the R_h values of freshly prepared PHSAM/GdW assemblies to be 70 nm at different $r<0.5$. After 24 h, only the assemblies with $r=0.5$ maintained $R_h=$ 70 nm even after 3 d (Figure S8), while the other assemblies with smaller r became a little bit larger (Figure 2). Furthermore, the concentration-dependent R_h results show that diluting the solution of assemblies with $r=0.5$ has little influence on the size of the assemblies (Figure S9). The zeta potential of PHSAM/GdW assemblies with $r=0.5$ is 50.6 mV, which is typical for stable colloid particles. Considering that a suitable Gd^{3+}-based MRI contrast agent needs to satisfy the requirement of both high content of Gd^{3+} ions and high stability, $r=0.5$ appears to be the optimal ratio to prepare PHSAM/GdW assemblies for MRI performance. In the following, assemblies with $r=0.5$ were investigated regarding their MRI performance and biocompatibility.

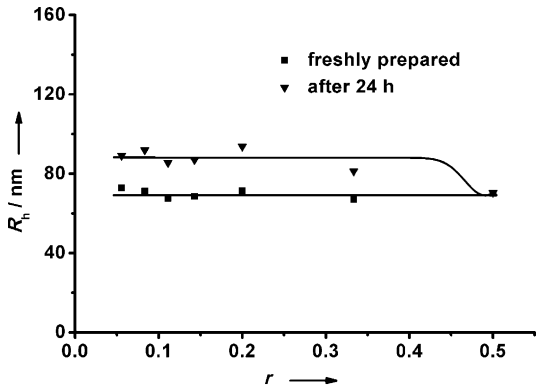

Figure 2. R_h values of the PHSAM/GdW assemblies prepared under the condition of different r and after different time.

SLS measurements were employed to further characterize the structure of the PHSAM/GdW assemblies. As shown in the Berry plot (Figure 3), the R_g value of PHSAM/GdW assemblies with $r=0.5$ is about 75 nm. The value of $R_g/R_h=$ 1.07 is larger than the theoretical value of 0.775 for monodisperse hard spheres, which may be caused by the polydis-

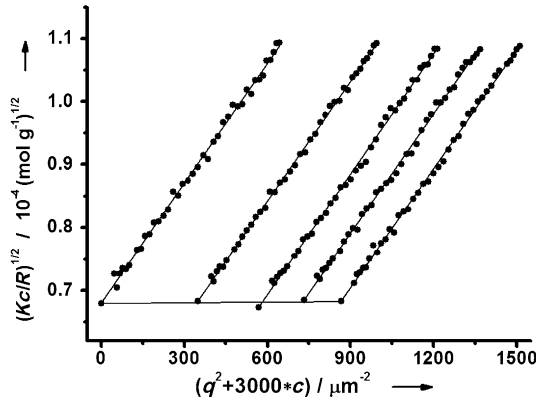

Figure 3. Berry plot of PHSAM/GdW assemblies with $r=0.5$ in water yielding $M_w=210\times10^6$ g mol^{-1}, $R_g=75$ nm, and the 2. virial coefficient $A_2=1.9\times10^{-7}$ mol L g^{-2}. The concentrations are 0.29, 0.24, 0.19 and 0.12 mg mL^{-1}; the refractive index increment is dn/d$c=0.1283$ cm^3 g^{-1}.

 © 2013 Wiley-VCH Verlag GmbH & Co. KGaA, Weinheim

persity of the assemblies. The solution density ρ of the assemblies may be estimated to $\rho = 0.25\ g\,cm^{-3}$ by utilizing $\rho = 3M_w/(4\pi N_A R_h^3)$ with the molar mass $M_w = 210 \times 10^6\ g\,mol^{-1}$, $R_h = 70$ nm, and $N_A =$ Avogadro number. Thus, the structures are swollen by approximately a factor of 4 by water, which allows bulk and GdW-coordinated water to exchange.

To further confirm the electrostatic interaction between PHSAM and GdW in the assemblies, X-ray photoelectron spectroscopy (XPS) was used to study the dry assemblies deposited on a silicon substrate. As shown in the N 1s spectra (Figure 4a), the binding energy of the nitrogen atoms of

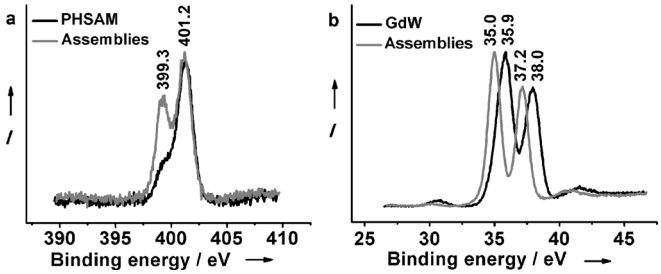

Figure 4. a) Contrast N 1s XPS spectra of PHSAM and PHSAM/GdW assemblies and b) contrast W 4f XPS spectra of GdW and PHSAM/GdW assemblies. The r values of all the assemblies are 0.5.

PHSAM is about 401.2 eV, corresponding to the ammonium bromide groups on the side chains of PHSAM. In contrast, the assemblies with $r = 0.5$ exhibit a new peak of N 1s besides 401.2 eV, appearing at a relatively low binding-energy position of 399.3 eV, which should be ascribed to the ammonium groups electrostatically interacting with GdW clusters. Since the charge ratio of GdW to PHSAM is 0.5 in the assemblies, only half of the positive charge of PHSAM is neutralized by GdW. Therefore, it is reasonable to observe both the free and the electrostatically bound ammonium groups in XPS spectra. On the other hand, in previous works we have found that the electrostatic encapsulation of tungsten-containing POMs by cationic surfactants can induce the W 4f peaks of POMs to shift to low-binding energy position, because the d^1 electrons in POMs become more difficult to delocalize.[11] For the PHSAM/GdW assemblies, a similar shift of the W 4f peaks was also observed in comparison with the pristine GdW (Figure 4b), which is another evidence for the electrostatic interaction between GdW and PHSAM.

In general, the stability of electrostatic assemblies is sensitive to the ionic strength of the ambient environment. Increasing the ionic strength can weaken the electrostatic interaction and destruct the assemblies. Therefore, it is important to evaluate the stability of PHSAM/GdW assemblies in a physiological environment containing abundant types of ions. For this purpose, we prepared PHSAM/GdW assemblies in an isotonic salt solution (150 mM NaCl). SLS results revealed the assemblies with $r = 0.5$ to be stable. The molar mass increased to $M_w = 300 \times 10^6\ g\,mol^{-1}$, the R_h and R_g values were both determined to 90 nm, also being somewhat larger as in water, but remained constant over a period of 3 d (Figures S10 and S11). The R_g/R_h value is, within experimental error, the same as in pure water, which indicates that the PHSAM/GdW assemblies prepared in pure water or in a 150 mM solution of NaCl have a similar structure, although the solution density is calculated to be somewhat smaller with $\rho = 0.15$.

It has been reported that Gd-POMs can accelerate the relaxation of water protons owing to the accommodation of paramagnetic Gd^{3+} ions in its framework, and thus, can serve as MRI contrast agents.[6] The contrast ability of Gd-POMs is influenced by several factors, such as molecular size, ambient hydrophobicity, and self-assembly behavior.[12] To investigate the influence of the microenvironment of PHSAM/GdW assemblies on the contrast ability of GdW, we compared the in vitro T_1-weighted MR images of GdW and PHSAM/GdW assemblies by using a clinical 1.5 T MR scanner at room temperature. As shown in row a in Figure 5, the images of GdW in water gradually become

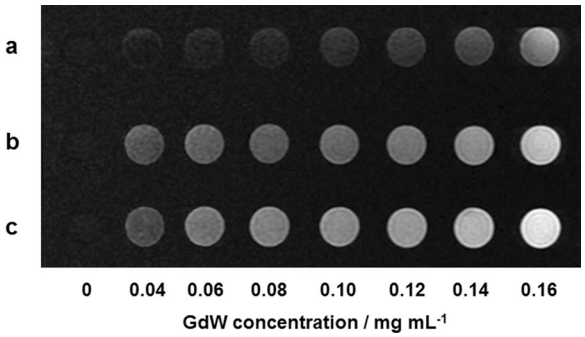

Figure 5. In-vitro T_1-weighted MR images of a) the aqueous solutions of GdW, b) the aqueous solutions, and c) the 150 mM solutions of PHSAM/GdW assemblies in NaCl with $r = 0.5$.

brighter with increasing concentration, which demonstrates the contrast ability of GdW. Enhanced contrasts are also observed for the PHSAM/GdW assemblies with $r = 0.5$ either in pure water or in the aqueous 150 mM solution of NaCl (row b and c in Figure 5) when the concentration of the assemblies is increased, indicating that the contrast ability of GdW is well maintained in the assemblies. It should be noted that the R_h values of the assemblies are stable in the varied concentration range (Figures S9 and S12). More importantly, the assemblies exhibit obviously brighter contrast images than the pristine GdW, which is consistent with the measured r_1 of GdW and PHSAM/GdW assemblies that are 4.6 and 13.7 $mM^{-1}S^{-1}$, respectively (Figure S13). Thus, the relaxivity of GdW is enhanced about 3 times in the assemblies. It has been reported that polymer micelles loaded with the clinically used gadopentetic acid (4.1 $mM^{-1}S^{-1}$) also showed a much higher relaxivity (48 $mM^{-1}S^{-1}$) than the free gadopentetic acid, because the restricted local motion of gadopentetic acid led to a prolongation of the rotational correlation time.[13] Therefore, we infer that the relaxivity enhancement of PHSAM/GdW assemblies is attributed to the

 © 2013 Wiley-VCH Verlag GmbH & Co. KGaA, Weinheim

longer rotational correlation time of GdW caused by the electrostatic interaction with PHSAM. Furthermore, the hydrophilic chains of PHASM may enable the external water molecules to freely penetrate the interior of the assemblies and to exchange with the coordinated water of GdW, since the spherical complexes are significantly swollen. The exchange between bulk and coordinated water of GdW also promotes the increase of r_1. The contrast intensity of PHSAM/GdW assemblies is similar in pure water and in the aqueous 150 mM solution of NaCl, demonstrating that the higher ionic strength has little influence on the MRI contrast of PHSAM/GdW assemblies.

The biocompatibility of PHSAM/GdW assemblies was tested by culturing HeLa cells and using the 3-(4,5-dimethylthiazol-2-yl)-2,5-diphenyltetrazolium bromide (MTT) assay. Results for different incubation times and concentrations are shown in Figure 6. The number of viable cells incubated with PHSAM/GdW assemblies after 48 h was close to 85%, even if the GdW concentration in the assemblies is as high as 0.16 mg mL^{-1}, indicating a good biocompatibility of the assemblies. It has been reported that the encapsulation of POMs into biocompatible polymer matrices, for example, chitosan, can lower the cell toxicity of POMs.[14] In the present work, PHSAM is a cationic polymer with compatible spermine groups as side chains. Therefore, spermine groups (though with a significantly reduced cationic charge) should be abundant on the surface of the PHSAM/GdW assemblies, which probably contributes to the low toxicity of assemblies.

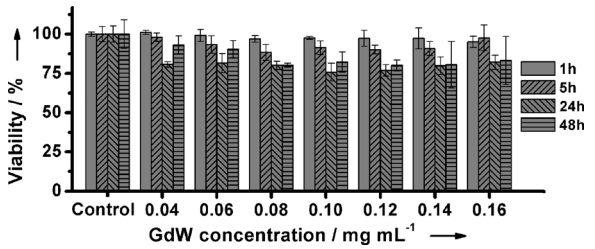

Figure 6. MTT assay of PHSAM/GdW assemblies with $r = 0.5$ in HeLa cells.

In conclusion, the cationic polymer PHSAM and anionic GdW clusters form hybrid assemblies by electrostatic interaction. The assemblies are stable in water and in isotonic salt solution. Importantly, the T_1-weighted MRI performance of GdW is enhanced about 3 times in the assemblies; meanwhile, the assemblies show good biocompatibility, which enables them to be promising candidates for MRI contrast agents. This work demonstrates that incorporation of POMs into water-penetrable and biocompatible polymer matrices is a promising strategy to fabricate POM-based MRI contrast agents. Other properties of POMs, such as luminescence,[15] anti-tumor, and anti-viral properties,[16] may also be optimized in such hybrid assemblies, which may lead to more POM-based biochemical applications.

Experimental Section

Preparation of PHSAM/GdW assemblies: GdW (26 mg) was dissolved in water (25 mL); PHSAM (7.8 mg) was dissolved in water (50 mL). Afterwards, 3.6 mL of the GdW solution were added droppwise into 20 mL of the PHSAM solution under stirring with a speed of 500 rpm. The mixture was stirred for further 0.5 h to obtain a mother solution of PHSAM/GdW assemblies in which the content of GdW is 0.16 mg mL^{-1}. The other solutions with different GdW contents were prepared by diluting the mother solution. For preparing assemblies in NaCl solution, just replace water with the aqueous solution of NaCl (150 mM).

Acknowledgements

The authors acknowledge the financial support from the National Basic Research Program (2013CB834503), the National Natural Science Foundation of China (91227110, 21274053), the 111 Project (B06009), and the Jilin Provincial Science & Technology Department (201201013) for supporting this cooperation.

Keywords: cationic polymers · hybrid materials · magnetic resonance imaging · polyoxometalates · self-assembly

[1] M. A. Brown, R. C. Semelka, *MRI: Basic Principles and Applications*, Wiley-Liss, Chichester, **2003**.
[2] A. J. L. Villaraza, A. Bumb, M. W. Brechbiel, *Chem. Rev.* **2010**, *110*, 2921–2959.
[3] a) S. Aime, M. Botta, M. Fasano, E. Terreno, *Chem. Soc. Rev.* **1998**, *27*, 19–29; b) P. Caravan, J. J. Ellison, T. J. McMurry, R. B. Lauffer, *Chem. Rev.* **1999**, *99*, 2293–2352; c) E. Terreno, D. D. Castelli, A. Viale, S. Aime, *Chem. Rev.* **2010**, *110*, 3019–3042; d) E. J. Werner, A. Datta, C. J. Jocher, K. N. Raymond, *Angew. Chem.* **2008**, *120*, 8696–8709; *Angew. Chem. Int. Ed.* **2008**, *47*, 8568–8580; e) A. Datta, K. N. Raymond, *Acc. Chem. Res.* **2009**, *42*, 938–947; f) P. Caravan, *Chem. Soc. Rev.* **2006**, *35*, 512–523; g) M. Bottrill, L. Kwok, N. J. Long, *Chem. Soc. Rev.* **2006**, *35*, 557–571.
[4] a) H. B. Na, T. Hyeon, *J. Mater. Chem.* **2009**, *19*, 6267–6273; b) A. Accardo, D. Tesauro, L. Aloj, C. Pedone, G. Morelli, *Coord. Chem. Rev.* **2009**, *253*, 2193–2213.
[5] a) M. T. Pope, A. Müller, *Angew. Chem.* **1991**, *103*, 56–70; *Angew. Chem. Int. Ed. Engl.* **1991**, *30*, 34–48; b) D. E. Katsoulis, *Chem. Rev.* **1998**, *98*, 359–388; c) D. L. Long, E. Burkholder, L. Cronin, *Chem. Rev. Soc.* **2007**, *36*, 105–121; d) D. L. Long, R. Tsunashima, L. Cronin, *Angew. Chem.* **2010**, *122*, 1780–1803; *Angew. Chem. Int. Ed.* **2010**, *49*, 1736–1758.
[6] a) J. Feng, X. Li, F. Pei, G. Sun, X. Zhang, M. Liu, *Magn. Reson. Imaging* **2002**, *20*, 407–412; b) Z. Li, W. Li, X. Li, F. Pei, Y. Li, H. Lei, *Magn. Reson. Imaging* **2007**, *25*, 412–417; c) M. Martínez-Pérez, O. Montero, M. Evangelisti, F. Luis, J. Sesé, S. Cardona-Serra, E. Coronado, *Adv. Mater.* **2012**, *24*, 4301–4305.
[7] L. Zheng, Y. Ma, G. Zhang, J. Yao, B. S. Bassil, U. Kortz, B. Keita, P. Oliveira, L. Nadjo, C. T. Craescu, S. Miron, *Eur. J. Inorg. Chem.* **2009**, 5189–5193.
[8] J. M. Lehn, *Proc. Natl. Acad. Sci. USA* **2002**, *99*, 4763–4768.
[9] a) D. G. Kurth, P. Lehmann, D. Volkmer, H. Cölfen, M. J. Koop, A. Müller, A. D. Chesne, *Chem. Eur. J.* **2000**, *6*, 385–393; b) T. Zhang, C. Spitz, M. Antonietti, C. F. J. Faul, *Chem. Eur. J.* **2005**, *11*, 1001–1009; c) H. Li, H. Sun, W. Qi, M. Xu, L. Wu, *Angew. Chem.* **2007**, *119*, 1322–1325; *Angew. Chem. Int. Ed.* **2007**, *46*, 1300–1303; d) A. Nisar, J. Zhuang, X. Wang, *Chem. Mater.* **2009**, *21*, 3745–3751; e) J. Zhang, Y. Liu, Y. Li, H. Zhao, X. Wan, *Angew. Chem.* **2012**, *124*, 4676–4680; *Angew. Chem. Int. Ed.* **2012**, *51*, 4598–4602.

 © 2013 Wiley-VCH Verlag GmbH & Co. KGaA, Weinheim

[10] S. Fluegel, J. Buehler, K. Fischer, J. R. McDaniel, A. Chilkoti, M. Schmidt, *Chem. Eur. J.* **2011**, *17*, 5503–5506.
[11] W. Bu, H. Li, W. Li, L. Wu, C. Zhai, Y. Wu, *J. Phys. Chem. B* **2004**, *108*, 12776–12782.
[12] Y. Wang, S. Zhou, D. Kong, H. Yang, W. Chai, U. Kortz, L. Wu, *Dalton Trans.* **2012**, *41*, 10052–10059.
[13] P. Mi, H. Cabral, D. Kokuryo, M. Rafi, Y. Terada, I. Aoki, T. Saga, I. Takehiko, N. Nishiyama, K. Kataoka, *Biomaterials* **2013**, *34*, 492–500.
[14] a) G. Geisberger, S. Paulus, M. Carraro, M. Bonchio, G. R. Patzke, *Chem. Eur. J.* **2011**, *17*, 4619–4625; b) G. Geisberger, S. Paulus, E. B. Gyenge, C. Maake, G. R. Patzke, *Small* **2011**, *7*, 2808–2814.
[15] T. Yamase, *Chem. Rev.* **1998**, *98*, 307–326.
[16] J. T. Rhule, C. L. Hill, D. A. Judd, R. F. Schinazi, *Chem. Rev.* **1998**, *98*, 327–358.

Received: July 5, 2013
Published online: November 9, 2013

 © 2013 Wiley-VCH Verlag GmbH & Co. KGaA, Weinheim